

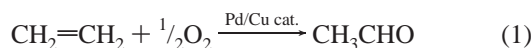
# Oxygenation of Nitrogen-Coordinated Palladium(0): Synthetic, Structural, and Mechanistic Studies and Implications for Aerobic Oxidation Catalysis

Shannon S. Stahl,\* Joseph L. Thorman, Ryan C. Nelson, and Michael A. Kozee

Department of Chemistry  
University of Wisconsin–Madison  
Madison, Wisconsin 53706

Received February 16, 2001  
Revised Manuscript Received June 6, 2001

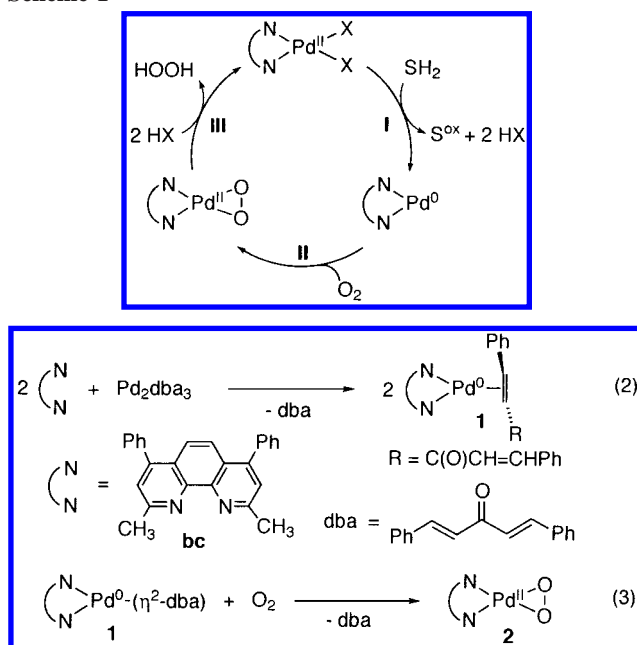
The palladium-catalyzed Wacker process (eq 1) was developed more than forty years ago<sup>1</sup> and remains one of the most successful aerobic oxidation reactions in the chemical industry. This process and numerous related reactions require cocatalysts such as copper salts to mediate dioxygen-coupled oxidation of reduced palladium during catalysis.<sup>2</sup> In contrast, a series of recent reports reveal that



cocatalysts are not always necessary to achieve efficient catalytic turnover.<sup>3</sup> Several of these new oxidation reactions employ a palladium catalyst with pyridine or bidentate nitrogen ligands,<sup>3a–c</sup> suggesting that such ligands promote the reaction between reduced palladium and dioxygen. A possible catalytic mechanism is shown in Scheme 1.<sup>3b,4,5</sup> We present herein the reaction between dioxygen and a bathocuproine–palladium(0) complex to form a structurally characterized peroxopalladium(II) species (step II, Scheme 1). This molecule reacts with Brønsted acids to release hydrogen peroxide (step III, Scheme 1). Bathocuproine (bc, 2,9-dimethyl-4,7-diphenyl-1,10-phenanthroline) has been used successfully in recent aerobic oxidation reactions.<sup>3b</sup> Mechanistic insights into the oxygenation of palladium(0) are also presented.

Due to the preference of palladium(0) for soft ligands, relatively few nitrogen-coordinated palladium(0) complexes have been reported.<sup>6</sup> Nevertheless, addition of 2 equiv of bathocuproine to tris(dibenzylideneacetone)dipalladium(0) in dichloromethane readily affords the orange, three-coordinate complex, (bc)Pd( $\eta^2$ -dba), **1** (eq 2), which was characterized by <sup>1</sup>H and <sup>13</sup>C NMR, IR, and UV–visible spectroscopies and single-crystal X-ray crystallography. The  $\eta^2$ -olefin ligand in **1** does not rotate or exchange on the NMR time scale; the <sup>1</sup>H NMR spectrum of **1** features two sharp singlets corresponding to the inequivalent bathocuproine

Scheme 1



methyl groups ( $\delta$  2.97, 3.21) and two doublets for the coordinated olefin protons ( $\delta$  4.47, 4.24, <sup>3</sup>J = 9.5 Hz).

The brown bathocuproine peroxopalladium(II) complex, **2**, was synthesized by stirring **1** in dichloromethane under an atmosphere of dry dioxygen for 20–30 min at ambient temperature (eq 3). Oxygenation of **1** is irreversible, revealed by the ability to isolate complex **2** by removal of the reaction solvent under vacuum. The <sup>1</sup>H NMR spectrum of **2** exhibits a single resonance for the bc methyl groups ( $\delta$  2.89), consistent with a symmetrical structure. The reaction was monitored by UV–visible spectroscopy (Figure 1) and revealed an isosbestic point at 393 nm suggesting no intermediates build up during the reaction.<sup>7</sup> The charge-transfer band for **1** in the 420 nm region is similar to that of other diimine palladium(0)–olefin complexes.<sup>6d</sup>

The presence of a peroxo moiety is supported by infrared spectroscopic data, which reveal a strong absorption band at 891 cm<sup>−1</sup>, similar to other late-transition-metal peroxo complexes.<sup>8</sup> The preparation of **2** with <sup>18</sup>O<sub>2</sub> results in a new band at 839 cm<sup>−1</sup> (Figure S1), corresponding to an isotopic shift of 52 cm<sup>−1</sup>, equal to the value predicted by a simple diatomic oscillator model for an O–O stretch. The  $\eta^2$ -peroxo coordination mode was established by single-crystal X-ray crystallography (Figure 2).<sup>9</sup> Only one other  $\eta^2$ -peroxopalladium complex, [Ph(*t*-Bu)<sub>2</sub>P]<sub>2</sub>Pd(O<sub>2</sub>), **3**, has been structurally characterized.<sup>8b</sup> Unlike (bc)Pd(O<sub>2</sub>), **3** binds

(7) The isosbestic behavior shown in Figure 1 arises a few minutes after initially placing the cuvette in the sample holder. Initial nonisosbestic behavior (not shown) has been traced to self-association of the (bc)Pd(dba) starting material; a nonlinear Beer's law plot is obtained for this species. The products of the oxygenation reaction, (bc)Pd(O<sub>2</sub>) and dba, appear to inhibit this self-association, evidenced by the subsequent isosbestic behavior. The lack of an intermediate in eq 3 was confirmed by monitoring the reaction by <sup>1</sup>H NMR spectroscopy.

(8) For peroxopalladium(II) complexes bearing soft donor ligands, see: (a) Valentine, J. S. *Chem. Rev.* **1973**, *73*, 235–245. (b) Yoshida, T.; Tatsumi, K.; Matsumoto, M.; Nakatsu, K.; Nakamura, A.; Fueno, T.; Otsuka, S. *Nouv. J. Chim.* **1979**, *3*, 761–774.

(9) Crystal data for **2**: monoclinic space group C2/c, *a* = 17.671(3) Å, *b* = 21.326(5) Å, *c* = 27.367(6) Å,  $\beta$  = 90.510(4)°, *V* = 10313(4) Å<sup>3</sup>, *Z* = 16, *T* = 133 K,  $\mu(\text{Mo K}\alpha)$  = 0.749 mm<sup>−1</sup>, 9034 unique reflections, *wR* = 0.3192, *R*[*I* > 2 $\sigma$ ] = 0.1054. The structure of **3** was redetermined at 173 K (cf. ref 8b, 248 K) in order to obtain improved structural resolution. Crystal data for **3**: orthorhombic space group P2<sub>1</sub>2<sub>1</sub>2<sub>1</sub>, *a* = 25.6846(8) Å, *b* = 12.2033(4) Å, *c* = 11.0834(3) Å, *V* = 3473.95(18) Å<sup>3</sup>, *Z* = 4, *T* = 173 K,  $\mu(\text{Mo K}\alpha)$  = 0.654 mm<sup>−1</sup>, 7011 unique reflections, *wR*[*I* > 2 $\sigma$ ] = 0.0756, *R*[*I* > 2 $\sigma$ ] = 0.0355.

(1) Smidt, J.; Hafner, W.; Jira, R.; Sedlmeier, J.; Sieber, R.; Rüttinger, R.; Kojer, H. *Angew. Chem.* **1959**, *71*, 176–182.

(2) Tsuji, J. *Palladium Reagents and Catalysts*; Wiley: New York, 1995.

(3) For leading references, see: (a) ten Brink, G.-J.; Arends, I. W. C. E.; Sheldon, R. A. *Science* **2000**, *287*, 1636–1639. (b) Bianchi, D.; Bortolo, R.; D'Aloisio, R.; Ricci, M. *Angew. Chem., Int. Ed.* **1999**, *38*, 706–708. (c) Nishimura, T.; Onoue, T.; Ohe, K.; Uemura, S. *J. Org. Chem.* **1999**, *64*, 6750–6755. (d) Peterson, K. P.; Larock, R. C. *J. Org. Chem.* **1998**, *63*, 3185–3189. (e) Rönn, M.; Andersson, P. G.; Bäckvall, J.-E. *Acta Chem. Scand.* **1997**, *51*, 773–777. (f) van Benthem, R. A. T. M.; Hiemstra, H.; van Leeuwen, P. W. N. M.; Geus, J. W.; Speckamp, W. N. *Angew. Chem., Int. Ed. Engl.* **1995**, *34*, 457–460.

(4) Thiel, W. R. *Angew. Chem., Int. Ed.* **1999**, *38*, 3157–3158.

(5) Alternative mechanisms have been proposed. These include dioxygen insertion into a palladium(II) hydride (ref 3c) and binuclear activation of dioxygen by 2 equiv of palladium(0) (ref 3a). We consider these possibilities less likely, but the present work does not necessarily exclude them.

(6) (a) Ito, T.; Hasegawa, S.; Takahashi, Y.; Ishii, Y. *J. Organomet. Chem.* **1974**, *73*, 401–409. (b) Pierpont, C. G.; Buchanan, R. M.; Downs, H. H. *J. Organomet. Chem.* **1977**, *124*, 103–112. (c) Sustmann, R.; Lau, J.; Zipp, M. *Recl. Trav. Chim. Pays-Bas* **1986**, *105*, 356–359. (d) van Asselt, R.; Elsevier, C. J.; Smeets, W. J. J.; Spek, A. L. *Inorg. Chem.* **1994**, *33*, 1521–1531. (e) Klein, R. A.; Elsevier, C. J.; Hartl, F. *Organometallics* **1997**, *16*, 1284–1291. (f) Milani, B.; Anzilutti, A.; Vicentini, L.; Sessanta o Santi, A.; Zangrando, E.; Geremia, S.; Mestroni, G. *Organometallics* **1997**, *16*, 5064–5075. (g) Elsevier, C. J. *Coord. Chem. Rev.* **1999**, *185–186*, 809–822.

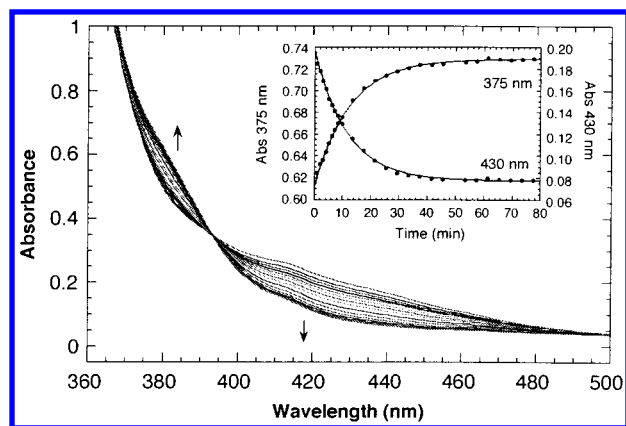


**Figure 1.** UV-visible absorption spectra obtained during the conversion of **1** to **2** in  $\text{CH}_2\text{Cl}_2$  (23 °C,  $p\text{O}_2 = 1$  atm,  $[\mathbf{1}] = 220 \mu\text{M}$ ). Inset: Kinetic data (●) at 375 and 430 nm with first-order fits to the data ( $t_{1/2} = 8.2(4)$  min).

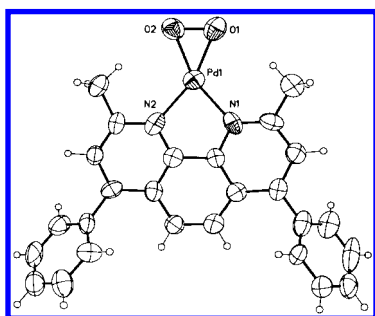


**Figure 2.** Molecular structure of (bc)Pd(O<sub>2</sub>), **2**. Thermal ellipsoids are drawn at 50% probability.

dioxygen reversibly, yet despite this reactivity difference, both complexes exhibit similar structural and spectroscopic features.<sup>10</sup>

It is reasonable to expect that the oxygenation of **1** should exhibit mechanistic similarities to reactions of other substrates with palladium(0) such as oxidative addition of aryl halides<sup>11</sup> or olefin substitution.<sup>6d,12</sup> These two reactions generally proceed by different mechanisms. Aryl halides typically add to a 14-electron  $\text{L}_2\text{Pd}(0)$  fragment that arises from endergonic ligand dissociation from a 16-electron species such as  $\text{L}_2\text{Pd}(\text{dba})$  ( $\text{L} = \text{phosphine}$ ), whereas olefin substitution reactions, e.g., by another olefin, are dominated by associative mechanisms in which tetrahedral, 18-electron intermediates are proposed.

Kinetic studies of the oxygenation reaction revealed a first-order dependence on dioxygen pressure (Figure 3), whereas addition of up to 10 equiv of dba had no effect on the rate (Figure S3). Activation parameters obtained from a temperature-dependence study revealed a substantial negative entropy of

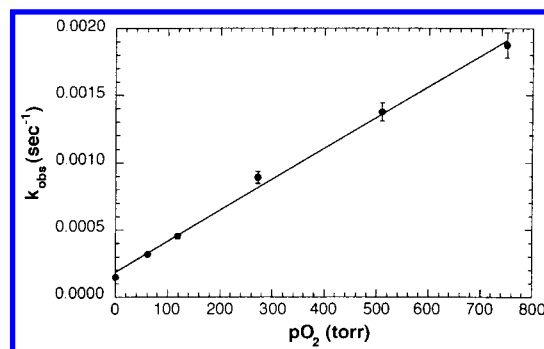


**Figure 3.**  $p\text{O}_2$  dependence on the formation of **2** from **1** and  $\text{O}_2$ . The nonzero y-intercept reflects a slow background decomposition of **1** in  $\text{CH}_2\text{Cl}_2$ .

activation,  $\Delta S^\ddagger = -43(7)$  eu. Together, these data support an associative oxygenation mechanism. The lack of inhibition by added dba rules out preequilibrium or steady-state loss of dba prior to dioxygen addition. Thus, although oxygenation of **1** represents a formal oxidative addition step, the reaction is mechanistically more closely related to olefin substitution.

As suggested in Scheme 1, substrate oxidation (step I) requires labile coordination sites on the palladium(II) catalyst. These sites may be created by protonolysis of the basic peroxo ligand in **2**. Addition of  $\text{CH}_3\text{CO}_2\text{H}$  or  $\text{H}_2\text{SO}_4$  to **2** quantitatively forms (bc)PdX<sub>2</sub> [ $\text{X}_2 = (\text{OAc})_2, \text{SO}_4$ ] based on  $^1\text{H}$  NMR analysis of the palladium species.<sup>13a</sup> A 73% yield of hydrogen peroxide was obtained via a colorimetric assay.<sup>13b,14</sup>

The chemistry described above demonstrates the chemical viability of steps II and III of the proposed mechanism in Scheme 1. Initial calculations suggest these steps are also kinetically competent to participate in the catalytic reactions;<sup>3b,15</sup> however, the reaction conditions are sufficiently different to warrant further investigation, especially in light of alternative mechanistic proposals.<sup>5</sup>

**Acknowledgment.** We gratefully acknowledge financial support from the University of Wisconsin–Madison, the Camille and Henry Dreyfus Foundation, and Merck Research Laboratories, and a generous donation of laboratory equipment by Abbott Laboratories. We appreciated crystallographic assistance from Dr. Ilia A. Guzei. The National Science Foundation provided financial support for NMR and X-ray instrumentation.

**Supporting Information Available:** Experimental procedures, spectroscopic data, kinetics data, and X-ray crystallographic tables for complexes **1**, **2**, and **3** (PDF). This material is available free of charge via the Internet at <http://pubs.acs.org>.

JA015683C

(10) Complex **2**,  $\nu_{\text{O-O}} = 891 \text{ cm}^{-1}$ ,  $d_{\text{O-O}} = 1.411(18) \text{ \AA}$  (average). Complex **3**,  $\nu_{\text{O-O}} = 916 \text{ cm}^{-1}$ ,  $d_{\text{O-O}} = 1.412(4) \text{ \AA}$ .

(11) (a) Amatore, C.; Jutand, A. *Coord. Chem. Rev.* **1998**, *178–180*, 511–528. (b) Alcazar-Roman, L. M.; Hartwig, J. F.; Rheingold, A. L.; Liable-Sands, L. M.; Guzei, I. A. *J. Am. Chem. Soc.* **2000**, *122*, 4618–4630. (c) Portnoy, M.; Milstein, D. *Organometallics* **1993**, *12*, 1665–1673.

(12) See, for example: (a) Cheng, P.-T.; Cook, C. D.; Nyburg, S. C.; Wan, K. Y. *Inorg. Chem.* **1971**, *10*, 2210–2213. (b) Ozawa, F.; Ito, T.; Nakamura, Y.; Yamamoto, A. *J. Organomet. Chem.* **1979**, *168*, 375–391. (c) Gómez-de la Torre, F.; Jálón, F. A.; López-Agenjo, A.; Manzano, B. R.; Rodríguez, A.; Sturm, T.; Weissensteiner, W.; Martínez-Ripoll, M. *Organometallics* **1998**, *17*, 4634–4644. (d) Klein, R. A.; Witte, P.; van Belzen, R.; Fraanje, J.; Goubitz, K.; Numan, M.; Schenk, H.; Ernsting, J. M.; Elsevier, C. J. *Eur. J. Inorg. Chem.* **1998**, 319–330. (e) Reid, S. M.; Mague, J. T.; Fink, M. J. *J. Organomet. Chem.* **2000**, *616*, 10–18.

(13) (a) An NMR tube was charged with **2** (10.46 mmol), 1,3,5-( $\text{Bu}$ )<sub>3</sub>- $\text{C}_6\text{H}_3$  as internal standard (2.66  $\mu\text{mol}$ ),  $\text{CH}_3\text{CO}_2\text{H}$  (40.2  $\mu\text{mol}$ ), and  $\text{CD}_2\text{Cl}_2$  (ca. 0.63 mL). The solution immediately turns light yellow. All (bc)Pd(O<sub>2</sub>) had been consumed and (bc)Pd(OAc)<sub>2</sub> (10.25  $\mu\text{mol}$ , 98% yield) was observed by  $^1\text{H}$  NMR after 5 min. (b) Literature procedures were utilized in the spectrophotometric detection of  $\text{H}_2\text{O}_2$  as peroxotitanyl species: (i) Eisenberg, G. M. *Ind. Eng. Chem. Anal. Ed.* **1943**, *15*, 327–328. (ii) Werner, W. U.S. Patent 4,908,323, 1990.

(14) This can be compared with other known Pt and Pd complexes: (a) Muto, S.; Ogata, H.; Kamiya, Y. *Chem. Lett.* **1975**, 809–812. (b) Muto, S.; Kamiya, Y. *Bull. Chem. Soc. Jpn.* **1976**, *49*, 2587–2589. (c) Muto, S.; Tasaka, K.; Kamiya, Y. *Bull. Chem. Soc. Jpn.* **1977**, *50*, 2493–2494.

(15) The temperature dependence of the oxygenation reaction (Figure S2) can be used to determine its rate under conditions comparable to those in the (bc)Pd(OAc)<sub>2</sub>-catalyzed oxidation of carbon monoxide (70 °C,  $p\text{O}_2 = 64$  atm). This rate,  $0.79 \text{ s}^{-1}$ , compares favorably with the maximum catalytic turnover frequency,  $0.16 \text{ s}^{-1}$  (ref 3b).